Free-breathing & ungated cardiac imaging using calibrationless manifold smoothness regularization

Sunrita Poddar[1], Xiaoming Bi[2], Dingxin Wang[2], Mathews Jacob[1]

[1]*University of Iowa,* [2] *Siemens Healthcare*

Synopsis: We introduce an image manifold smoothness regularization, coupled with spatial regularization, for high-resolution free-breathing and ungated cardiac cine imaging. Prior work in this area relied on additional navigators within each image frame to estimate the manifold structure. In this abstract, we focus on eliminating the need for navigators, which will provide improved sampling efficiency.

Purpose: Functional cardiac CINE imaging is often performed with breath-holds to freeze cardiac motion. This is infeasible for many patients who cannot perform breath-holding. The breath-held protocol with intermittent pauses also results in long scan-time and restricts patient throughput. Single-shot schemes can be used, but the achievable spatial/temporal resolution is limited. Thus, there is an urgent clinical need for a free breathing ungated cardiac CINE protocol.

Methods: We extend the image manifold smoothness regularization (STORM)[1] scheme, where the similarity of images at the same cardiac/respiratory phases was exploited. STORM was enabled by a modified golden angle acquisition, where 3-4 spokes are acquired at the same k-space locations every frame. The measurement for the i^{th} image frame is specified by

$$\underbrace{\begin{bmatrix}\mathbf{z}_i \\ \mathbf{y}_i\end{bmatrix}}_{\mathbf{b}_i} = \underbrace{\begin{bmatrix}\mathbf{\Phi} \\ \mathbf{B}_i\end{bmatrix}}_{\mathbf{A}_i} \mathbf{x}_i + \mathbf{n}_i, \qquad [1]$$

where $\mathbf{z}_i$ denotes the common/navigator measurements. $\mathbf{y}_i$ are the measurements that are different from every frame. The Laplacian of the image manifold $\mathbf{L}$ is estimated from navigator data ($\mathbf{Z} = \mathbf{\Phi}\mathbf{X}$) as $\mathbf{L} = \mathbf{D} - \mathbf{W}$, where

$$\mathbf{W}_{i,j} = \exp\left(-\|\mathbf{z}_i - \mathbf{z}_j\|^2/\sigma^2\right); \quad \mathbf{D} = \text{diag}(\mathbf{1}^T\mathbf{W}). \qquad [2]$$

While STORM exploits the non-local similarities between images in the time series, it fails to capture the redundancies within each image. We improve STORM by adding a spatial total variation prior:

$$\mathbf{X}^* = \arg\min_{\mathbf{X}} \left\{\|\mathcal{A}(\mathbf{X}) - \mathbf{b}\|_F^2 + \lambda_1 \text{ trace}\left(\mathbf{X}\mathbf{L}\mathbf{X}^H\right) + \lambda_2 \|\mathbf{T}\mathbf{X}\|_{\ell_1}\right\}. \qquad [3]$$

Here, $\mathbf{T}$ is the spatial gradient matrix. We use FISTA [2] to solve the above optimization scheme.

We now introduce a technique (illustrated in Fig. 1) to estimate the weight matrix $\mathbf{W}$, when navigators are not available. We split the radial spokes in the entire golden angle acquisition to K groups, denoted by G_k, each of size $180/K$ degrees. We evaluate approximate weight matrices $\mathbf{W}^{(k)}; k = 1, .., K$ by comparing spokes in the images that are in the k^{th} group:

$$\mathbf{W}_{i,j}^{(k)} = \frac{1}{N_{ij}^k} \sum_{\{\mathbf{l}_m^{(i)}, \mathbf{l}_n^{(j)} \in G_k\}} \exp\left(-\|\mathbf{l}_m^{(i)} - \mathbf{l}_n^{(j)}\|^2/\sigma^2\right) \qquad [4]$$

Here, $\mathbf{l}_m^{(i)}$ and $\mathbf{l}_n^{(j)}$ are spokes in the i^{th} and j^{th} image frames, which are in group G_k. $N_{i,j}^k$ denotes total number of spoke pairs in k^{th} group between frames i and j. If there is no pair of spokes between two image frames, the corresponding weight is set to zero. The complete weight matrix is calculated as

$$\mathbf{W} = \frac{1}{N}\sum_{k=1}^{N} \mathbf{W}^{(k)} \qquad [5]$$

To prevent oversmoothing, $\mathbf{W}$ is post-processed to keep only 3-5 neighbours per frame.

Results: We demonstrate our scheme on 2 free-breathing ungated cardiac datasets, acquired using a FLASH sequence on a 3T scanner (MAGNETOM Skyra, Siemens Healthcare, Germany). Both were reconstructed using STORM and further processing was done using spatial TV.The first dataset had 10 radial spokes per frame, out of which 4 were navigator spokes. The sequence parameters were: TR/TE 4.3/1.92 ms, FOV 300mm, Base resolution 256, Bandwidth 574 Hz/pix. 10000 spokes of k-space were collected in 43 s. Fig. 3 shows a few reconstructed image frames where the weights were computed using navigator spokes. The second dataset was acquired with a golden angle ordering (no navigators). The sequence parameters were: TR/TE 3.7/1.67 ms, FOV 300mm, Base resolution 256, Bandwidth 977 Hz/pix. 11994 spokes of k-space were acquired in 44s and we used 13 spokes to reconstruct each image frame. The spokes were divided into 20 angle groups. Fig. 4 shows a few reconstructed image frames using the proposed scheme. We also show a reconstruction when only the temporal neighbours of each frame are assigned non-zero weights equal to 1.

Discussion: We note that spatial TV regularization reduces noise and streaking artefacts. It is seen that temporal regularization is insufficient to achieve good image quality. This motivates our proposed scheme. We observe that the image quality obtained with the navigator data is superior. This is because of the simple nature of the heuristic used to estimate the weights in the navigatorless case. We will explore more sophisticated kernel completion methods[3] to improve the weight evaluation in the calibrationless setting. This can make navigatorless reconstructions better than those with navigators due to increased incoherence in sampling patterns.

Conclusion: Spatial regularization is complementary to image manifold regularization which exploits the non-local similarities between image frames in a time series. The combination of the priors provides improved results. The heuristic approach to estimating the weights from calibrationless data shows promise; more work is required to improve the estimation of the manifold structure in cases without navigators.

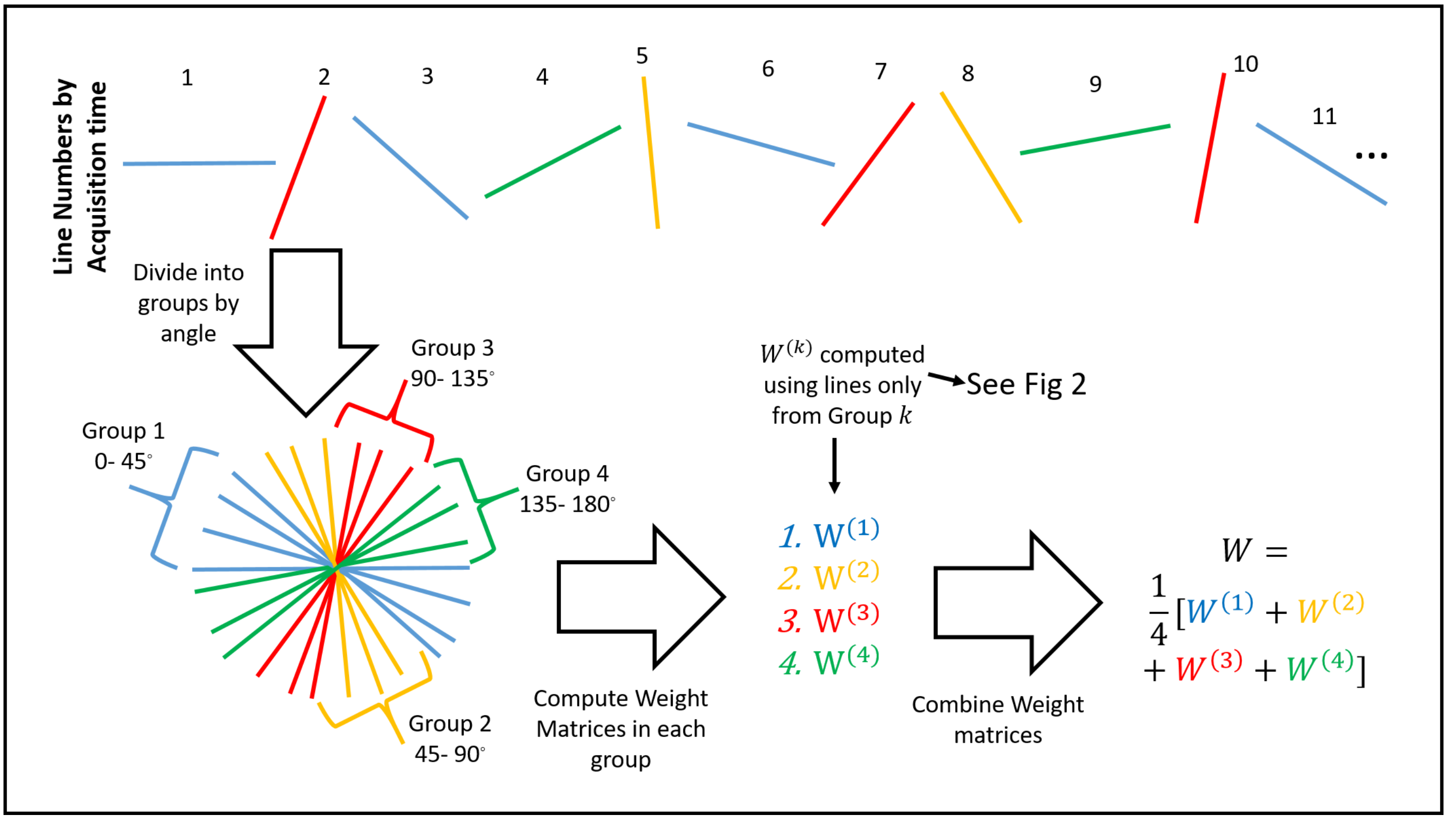

Figure 1: Summary of weight estimation without navigators: The sequence of radial spokes are shown arranged by the order in which they were acquired. The spokes are now grouped according to their angle. Here 4 groups have been illustrated. Weight matrices are estimated for each group. These are then averaged to form the final weight matrices.

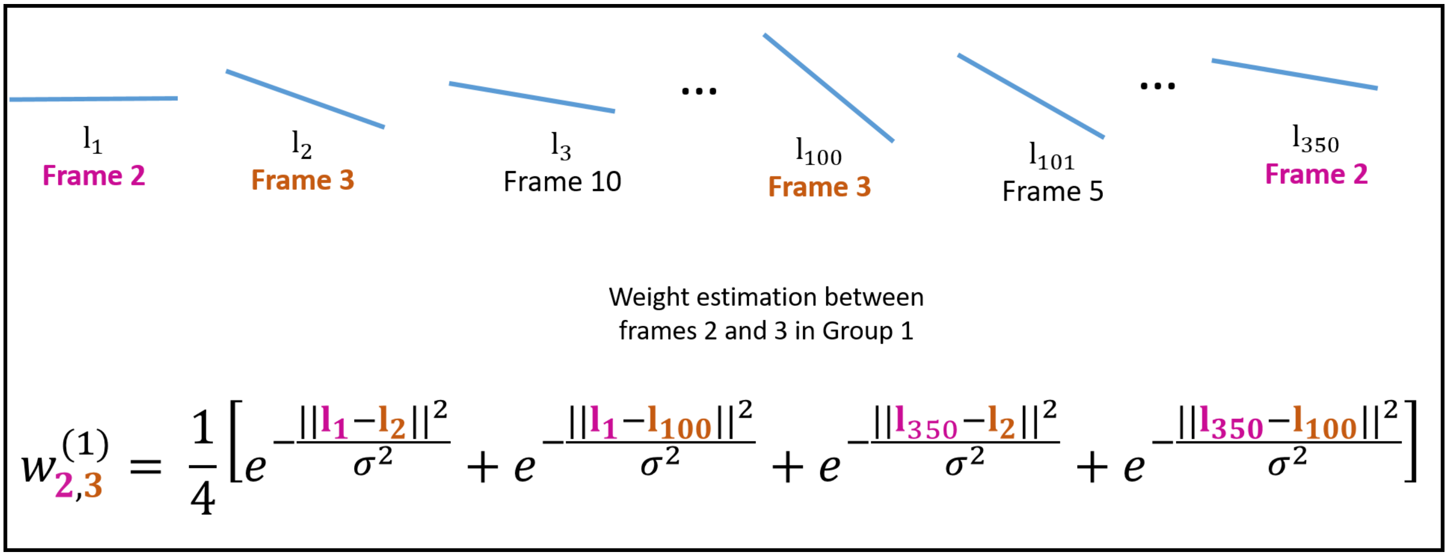

Figure 2: Group-wise weight estimation: As an example it is illustrated how the weight matrix for group 1 is estimated. The spokes are shown is blue as they come from group1 of Fig 1. In order to compute the weight between frames 2 and 3 for group 1, we require spokes 1 and 350 (from frame 2) and 2 and 100 (from frame 3).

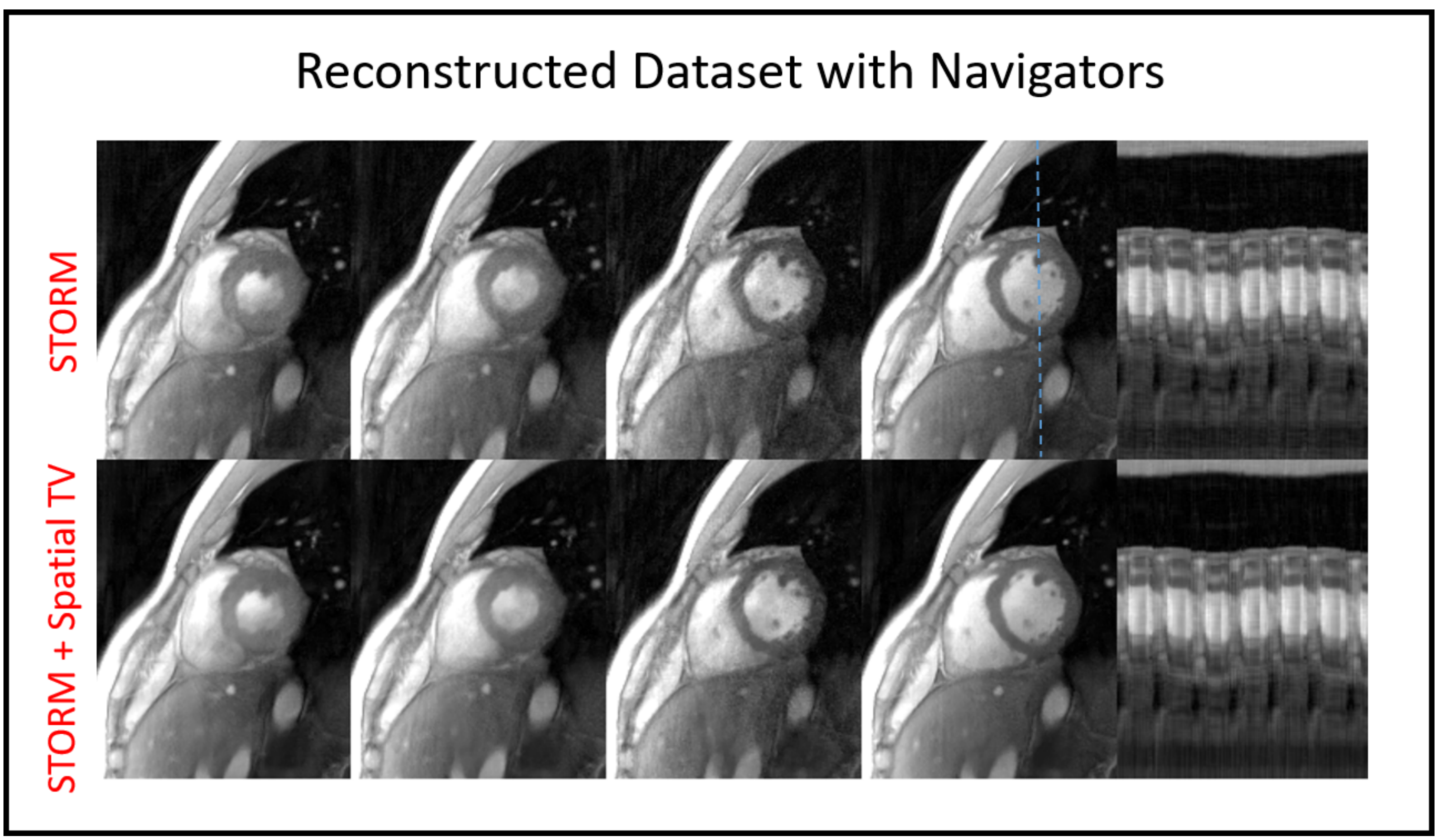

Figure 3: Reconstructions using navigators: The top row shows reconstructed images using the STORM algorithm, where the weights were computed using the navigator spokes. The bottom row shows reconstructed images with the above images as initial guess and 10 FISTA iterations which perform spatial TV regularization. The temporal profiles along the dotted blue line are also shown for both the reconstructed datasets.

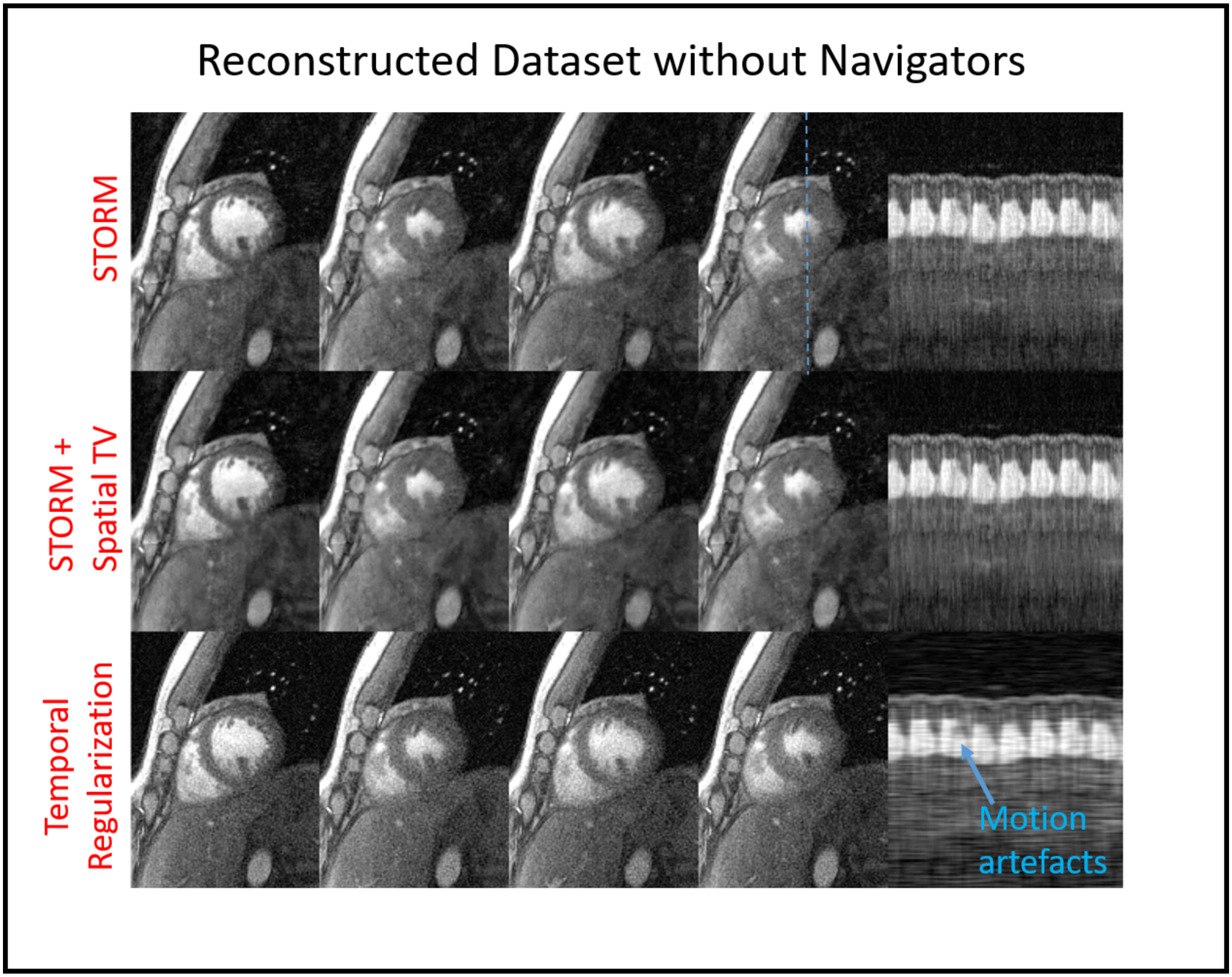

Figure 4: Reconstructions without navigators: The top row shows reconstructed images using the STORM algorithm, where the weights were computed using the proposed method. The bottom row shows reconstructed images with the above images as initial guess and 10 FISTA iterations which perform spatial TV regularization. The temporal profiles along the dotted blue line are also shown for both the reconstructed datasets.